The peculiar size and temperature dependence of water diffusion in carbon nanotubes studied with 2D NMR diffusion–relaxation $D–T_{2eff}$ spectroscopy 🄵 🅂🄲🄸

🆔 L. Gkoura, 🆔 G. Diamantopoulos, M. Fardis, 🆔 D. Homouz, 🆔 S. Alhassan, M. Beazi-Katsioti, 🆔 M. Karagianni, A. Anastasiou, 🆔 G. Romanos, 🆔 J. Hassan, and 🆔 G. Papavassiliou

COLLECTIONS

🄵   This paper was selected as Featured

🅂🄲🄸   This paper was selected as Scilight

View Online   Export Citation   CrossMark

ARTICLES YOU MAY BE INTERESTED IN

Confined in a narrow channel, water separates into sheets with peculiar properties
Scilight **2020**, 251108 (2020); https://doi.org/10.1063/10.0001492

Water above the spinodal
The Journal of Chemical Physics **152**, 174501 (2020); https://doi.org/10.1063/5.0006431

Updates to water's equation of state hold the key to describing its anomalous behaviors
Scilight **2020**, 191103 (2020); https://doi.org/10.1063/10.0001252

The peculiar size and temperature dependence of water diffusion in carbon nanotubes studied with 2D NMR diffusion–relaxation D–T_{2eff} spectroscopy ⓈⒸⒾ Ⓕ

L. Gkoura,[1] ⓘ G. Diamantopoulos,[1,2] ⓘ M. Fardis,[1] D. Homouz,[2,3,4] S. Alhassan,[5] ⓘ M. Beazi-Katsioti,[6]
M. Karagianni,[1] ⓘ A. Anastasiou,[1] G. Romanos,[1] ⓘ J. Hassan,[2,a)] ⓘ and G. Papavassiliou[1,a)] ⓘ

AFFILIATIONS

[1]Institute of Nanoscience and Nanotechnology, NCSR Demokritos, 15310 Aghia Paraskevi, Attiki, Greece
[2]Department of Physics, Khalifa University of Science and Technology, 127788 Abu Dhabi, UAE
[3]Department of Physics, University of Houston, Houston, Texas 77204-5005, USA
[4]Center for Theoretical Biological Physics, Rice University, Houston, Texas 77030-1402, USA
[5]Department of Chemical Engineering, Khalifa University of Science and Technology, 127788 Abu Dhabi, UAE
[6]School of Chemical Engineering, National Technical University of Athens, 15780 Zografou, Athens, Greece

[a)]**Authors to whom correspondence should be addressed:** jamal.hassan@ku.ac.ae and g.papavassiliou@inn.demokritos.gr

ABSTRACT

It is well known that water inside hydrophobic nano-channels diffuses faster than bulk water. Recent theoretical studies have shown that this enhancement depends on the size of the hydrophobic nanochannels. However, experimental evidence of this dependence is lacking. Here, by combining two-dimensional nuclear magnetic resonance diffusion–relaxation (D–T_{2eff}) spectroscopy in the stray field of a superconducting magnet and molecular dynamics simulations, we analyze the size dependence of water dynamics inside Carbon Nanotubes (CNTs) of different diameters (1.1–6.0 nm), in the temperature range of 265–305 K. Depending on the CNT diameter, the nanotube water is shown to resolve in two or more tubular components acquiring different self-diffusion coefficients. Most notably, a favorable CNT diameter range (3.0–4.5 nm) is experimentally verified for the first time, in which water molecule dynamics at the center of the CNTs exhibits distinctly non-Arrhenius behavior, characterized by ultrafast diffusion and extraordinary fragility, a result of significant importance in the efforts to understand water behavior in hydrophobic nanochannels.

Published under license by AIP Publishing. https://doi.org/10.1063/5.0005398

I. INTRODUCTION

The study of water diffusion inside Carbon Nanotubes (CNTs) has attracted great interdisciplinary interest as a conduit for understanding nanofluidic properties in a variety of nanoporous systems having potential in many applications, such as water treatment technologies,[1] drug delivery,[2,3] intracellular solute transport control,[4] and energy storage systems.[5,6] Theoretical methods, mostly Molecular Dynamics (MD) simulations,[2,7,8] have been used to investigate the structure and dynamics of water molecules inside CNTs. A major outcome of these studies is that water molecules tend to stratify in coaxial tubular sheets inside CNT channels.[7,9,10]

In certain CNT sizes, nanotubular water diffuses faster than bulk water[7,11,12] upon confinement. This fast water motion has been explained by several authors as due to H-bond modifications in the hydrophobic nanochannels or due to geometrical constraints and curvature induced incommensurability between the water and the CNT walls.[7] From the experimental point of view, a great number of methods, such as infrared spectroscopy,[13] Raman spectroscopy,[14,15] thermogravimetric analysis,[16] Transmission Electron Microscopy (TEM),[17–21] neutron scattering,[22–27] dielectric spectroscopy,[28] x-ray Compton scattering,[29–31] and Nuclear Magnetic Resonance (NMR)[32–35] have been widely used in the study of

molecular confinement and transport through the CNT channels.[36] However, until now, there is scarce experimental evidence at molecular scale, regarding the way water organizes and diffuses inside the CNTs, and the way these properties vary as a function of the channel size and temperature. These challenges are associated with a fundamental problem in the physics of soft matter, which is still not well understood, i.e., the microscopic origin of the temperature dependence of the structural and dynamic properties, such as structural relaxation times and transport coefficients, of confined liquids (see, for example, Ref. 37). The manifestation of a non-Arrhenius behavior in the temperature dependence of both the translational and rotational dynamics of liquid water has led Angel to introduce the concept of fragility, a useful classification of liquids along a strong and fragile scale.[37] According to this conception, a pure Arrhenius behavior classifies a strong liquid whereas a non-Arrhenius one signifies a fragile behavior. This is demonstrated, for example, in the supercooled state of water where an increase of the apparent activation energy is observed upon cooling, noticeable even at room temperature. Water confined in nanotubes exhibits similar phenomena as described in this work. In the above context, NMR is an important noninvasive tool with atomic scale resolution for studying water-surface and nano-confined water systems. Standard NMR experiments typically include longitudinal T_1, transverse T_2 relaxation times, self-diffusion coefficient D, and line shape measurements. In a recent survey[36] of NMR studies on the water dynamics inside CNTs, it is revealed that the majority of the published reports[38–42] focused on ^{1}H-water NMR-line shape vs temperature in order to establish the freezing point of the confined water. However, any change in the water structure and dynamics induced by the nano-confinement is expected to be also reflected in the ^{1}H NMR T_1, T_2, and D values of the water molecules. Such measurements for water-in CNTs have been rarely published.[43,44]

In this paper, we utilize two-dimensional ^{1}H NMR diffusion–relaxation correlation spectroscopy D–T_{2eff}[45–48] to study water confinement in CNTs as a function of size (1.1–6.0 nm) and temperature (265–305 K). In addition, MD simulations on the same systems were carried out in order to acquire the way that water is organized inside the CNTs and compare theoretical with experimental D values. Notably, in the CNT diameter range 3.0 nm–4.5 nm, water is shown to split into coaxial water tubular sheets (WTSs), with the central one obtaining an order of magnitude higher D, in comparison to the outer WTS close to the CNT wall. Even more, water molecules along the CNT axis show remarkable deviation from the Arrhenius temperature dependence; a very fragile, almost liquid-like axial water component, persisting even at very low temperatures, is formed, with fragility sufficiently higher than that of the bulk water.

II. RESULTS AND DISCUSSION

The water structure inside the CNTs varies upon increasing the CNT diameter; it forms a 1D chain of water molecules in ultra-narrow single-walled CNTs ($d < 1$ nm), and it is organized into coaxial WTS as the CNT diameter increases. Figure 1 shows three MD simulation snapshots of water configuration at room temperature inside CNTs with diameters 1.1 nm, 3.0 nm, and 5.0 nm.

In all three cases, water molecules inside CNT channels are shown to arrange in concentric WTS (circles in the snapshot), in agreement with previous publications (see, for example, Alexiadis and Kassinos,[10] and references therein). The number of WTS that can be accommodated inside CNT channels depends on the size of the CNTs and on the oxygen–oxygen as well as oxygen–carbon interactions.[10] It is furthermore observed that the stratified water arrangement into WTS becomes denser by increasing the CNT size and gradually the dynamics of water molecules approach that of bulk water.[10]

In order to verify experimentally the role of the CNT diameter on the water structure and dynamics, we conducted 2D ^{1}H NMR D–T_{2eff} measurements of water in various CNT sizes, ranging from 1.1 nm to 6.0 nm, and in the temperature range 265–305K. Experiments were performed in the stray field of a superconductive magnet with a constant magnetic field gradient $g = 34.7$ T/m, at ^{1}H NMR frequency of 101.324 MHz. It is noticed that in a constant strong magnetic field gradient, as in our case, the CPMG spin-echo decay curves, assigned to the T_2-axis,[45,49] decay with an effective T_{2eff}, which is sufficiently shorter than the intrinsic T_2 in the absence of a magnetic field gradient. For example, T_{2eff} of bulk

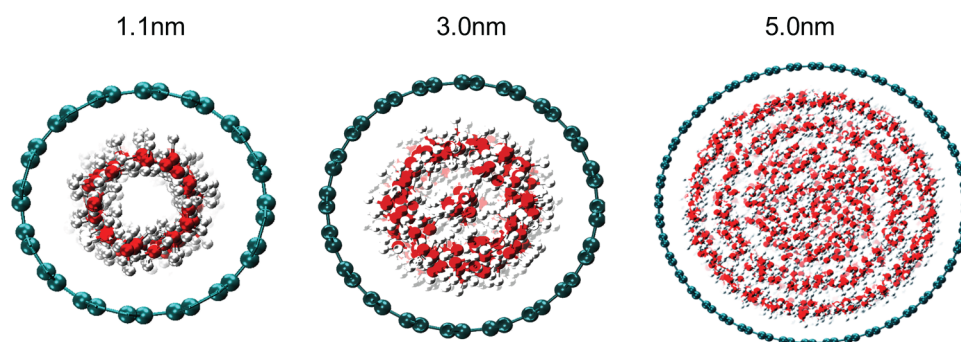1.1nm   3.0nm   5.0nm

FIG. 1. Snapshots from MD simulations of water molecules arrangements inside CNT nanotubes of different sizes (green: carbon atoms of the CNT wall, red: oxygen atoms, and white: hydrogen atoms. Circles represent different water layers).

water was found to be approximately 10 ms, instead of $T_2 \sim 2$ s in a homogeneous external magnetic field. Henceforth, the 2D diffusion–relaxation spectra refer to $D–T_{2eff}$ instead of $D–T_2$. Detailed discussion on this is given in the second section of the supplementary material.

In the case of NMR diffusion experiments with a uniform diffusion process, the self-diffusion coefficient D is obtained by appropriate fitting the ^{1}H NMR spin-echo decay data.[48] However, in non-uniform diffusion processes, diffusion is expressed with a distribution function $f(D)$, which can be obtained by implementing an appropriate inversion algorithm, as explained in the supplementary material. The advantage of the $D–T_{2eff}$ spectroscopy in comparison to 1D NMR diffusion measurements is its ability to resolve signals with different T_{2eff} and therefore acquire distinctly—otherwise overlapping—D values.[45] Consequently, D of the nanotube water can be resolved by analyzing the spin-echo decay signals in different T_{2eff} windows.

Figure 2 shows the 2D NMR $D–T_{2eff}$ spectra of four characteristic samples measured in this study, at 270 K and 285 K. The intensities of the NMR contour plots are rescaled accordingly to improve visualization. Two main signals are visible acquiring different T_{2eff} values, i.e., 0.5 ms and 10 ms, respectively. The short T_{2eff} signal is assigned to the nanotube water,[45] while the long T_{2eff} signal is assigned to bulk and interstitial water, i.e., external water confined in the space between CNTs, which are assembled in CNT-bundles, as explained in detail in Ref. 46. Upon lowering the temperature, bulk water freezes and the intensity of the NMR signal from the external water decreases rapidly, as observed in Fig. 5 of the supplementary material. Below 273 K, bulk water becomes invisible due to the extremely low $T_2 \approx T_{2eff}$ of ice and only the nanotube and interstitial water are observed.

To uncover the nanotube water dynamics, we calculated separately the D projections corresponding to the short T_{2eff} signal component, i.e., to the nanotube water. Figure 3 shows the diffusion profile of the nanotube water for all measured samples at

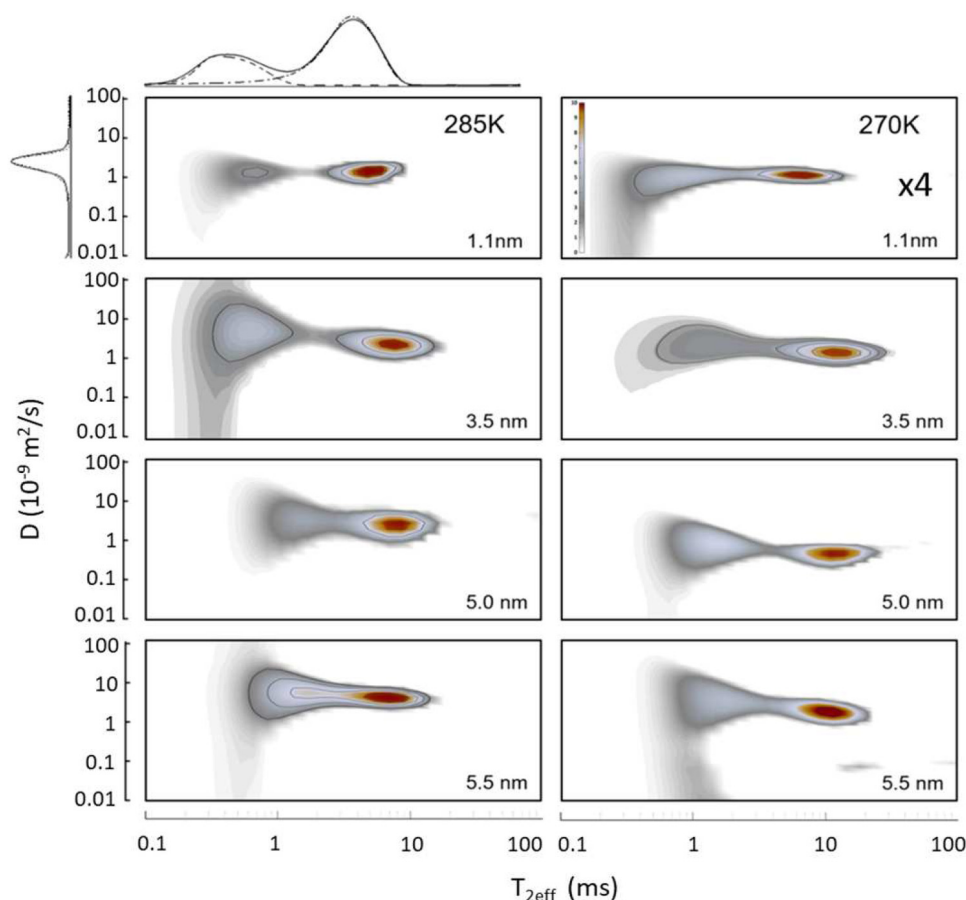**FIG. 2.** 2D ^{1}H NMR $D–T_{2eff}$ contour plots of water inside CNT of sizes 1.1 nm, 3.5 nm, 5.0 nm, and 5.5 nm, at selected temperatures (270 K and 285 K). Two main T_{2eff} peaks are observed, corresponding to two different water groups (interstitial and nanotube water)—as seen in the T_{2eff} projection for a 1.1 nm sample at 285 K. For better visualization, all signal intensities at 270 K are multiplied by 4.
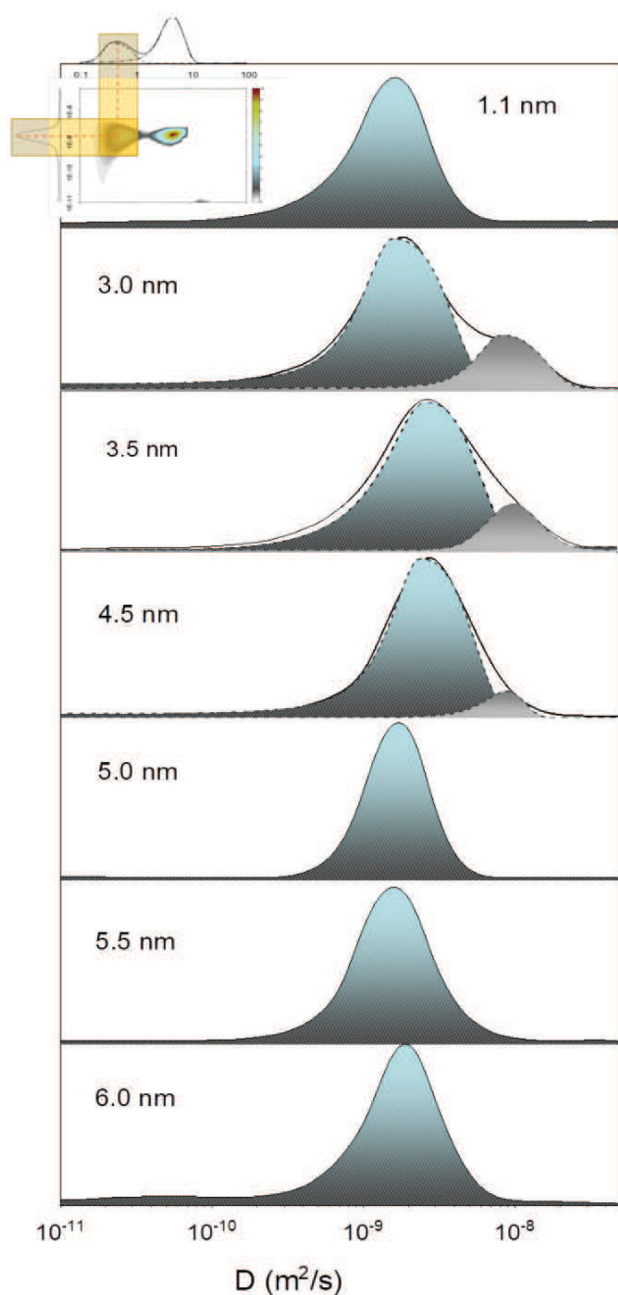
FIG. 3. ^{1}H NMR diffusion projections (solid lines) from the D–T_{2eff} spectra of the internal nanotube water in different CNT sizes at 285 K. Diffusion projections at certain CNT sizes (3.0 nm, 3.5 nm, and 4.5 nm) are resolved into two components (dashed curves), represented by the main and the shoulder peaks.

285 K. In all temperatures, the diffusion curves acquire an asymmetric distribution with a long tail toward the low D values, which is the fingerprint of uniform 1D restricted diffusion in a set of randomly oriented nanochannels.[45,50] Remarkably, the diffusion

profiles at certain CNT sizes (3.0 nm, 3.5 nm, and 4.5 nm) can be fitted with two log-norm distribution functions, with the faster one exhibiting D values up to five times higher than that of bulk water. Furthermore, in the same CNT size range, the D values of the main diffusion peak are sufficiently higher than those of the rest CNT sizes. For instance, it is found that $D \sim 2.6 \times 10^{-9}\,\mathrm{m^2/s}$ in the 3.5 nm CNT, sufficiently faster than $D \sim 1.6 \times 10^{-9}\,\mathrm{m^2/s}$ in the 5.5 nm sample. This result is in agreement with previous studies,[43,51] which show that the mean D value of water in small CNT sizes is twice as large than in large CNT sizes. At larger CNT diameters, D acquires the value of bulk water. In order to understand the split of water dynamics in two components, MD simulations were conducted at room temperature in different sizes of CNTs, to reveal the local density of the water layers and the diffusion coefficients. Results are presented in Fig. 4. The stratified water arrangement is clearly seen within the CNTs. In a small CNT size of 1.1 nm, water molecules form a single tubular layer in agreement with the literature.[7] Due to the hydrophobic interaction between water molecules and carbon atoms of the CNT walls, water molecules of this layer are far from the CNT wall by 0.3 nm. Furthermore, the calculated D values are about $\sim 0.7 \times 10^{-9}\,\mathrm{m^2/s}$ as seen in Fig. 4.

Upon increasing the CNT diameter, additional water-layers are formed. In the 3.0 nm size sample, MD simulations reveal two concentric WTS with different D values in agreement with the NMR results. The water density profiles indicate that the outer WTS close to the CNT wall corresponds to the main diffusion peak in Fig. 3, while the central WTS corresponds to the fast diffusion component. The outer WTS shows a mean D value of approximately $2.2 \times 10^{-9}\,\mathrm{m^2/s}$, in agreement with the NMR results; however, the central WTS differs significantly from the experimentally measured D value at the center of the CNT channel. Finally, in the large diameter sample (5.0 nm), although the MD simulation has revealed multiple water layers, their calculated D values are close to each other, unveiling uniform dynamics across the diameter, in agreement to the NMR results of Fig. 3. Similar analysis was performed to all samples at various temperatures. At this point, it is important to rule out the diffusion of water molecules in the radial direction of the CNT channels. This is due to the large free-energy-barrier between consecutive layers in the radial direction, which might take values as high as 1–2 kcal/mol.[10] We have examined the diffusion mechanism of water inside CNTs in both directions: radial and axial. In our simulations, we see that the diffusion in the radial direction is several orders of magnitudes smaller than that in the axial direction. Therefore, radial diffusion is prohibited especially at low temperatures, where molecules do not have sufficient thermal energy to overcome the free energy barrier.

Figure 5 shows the temperature dependence of the inverse of the self-diffusion coefficient $1/D$ vs $1000/T$, of the nanotube water in CNTs with diameter ranging from 1.1 nm to 6.0 nm, in the temperature range of 265–305 K. The blue lines are the relevant curves of an ideal liquid obeying the Arrhenius law $\frac{1}{D} = \frac{1}{D_0}\exp\left(\frac{U}{k_B T}\right)$ for two different initial $1/D_0$ values. Such liquids are denoted in the literature as strong liquids.[52] The yellow circles are the experimental values of bulk water; at high temperatures, water follows the Arrhenius law; however, as shown in Fig. 5, below the liquidus temperature $T_l \approx 273$ K, i.e., the temperature above which a material is
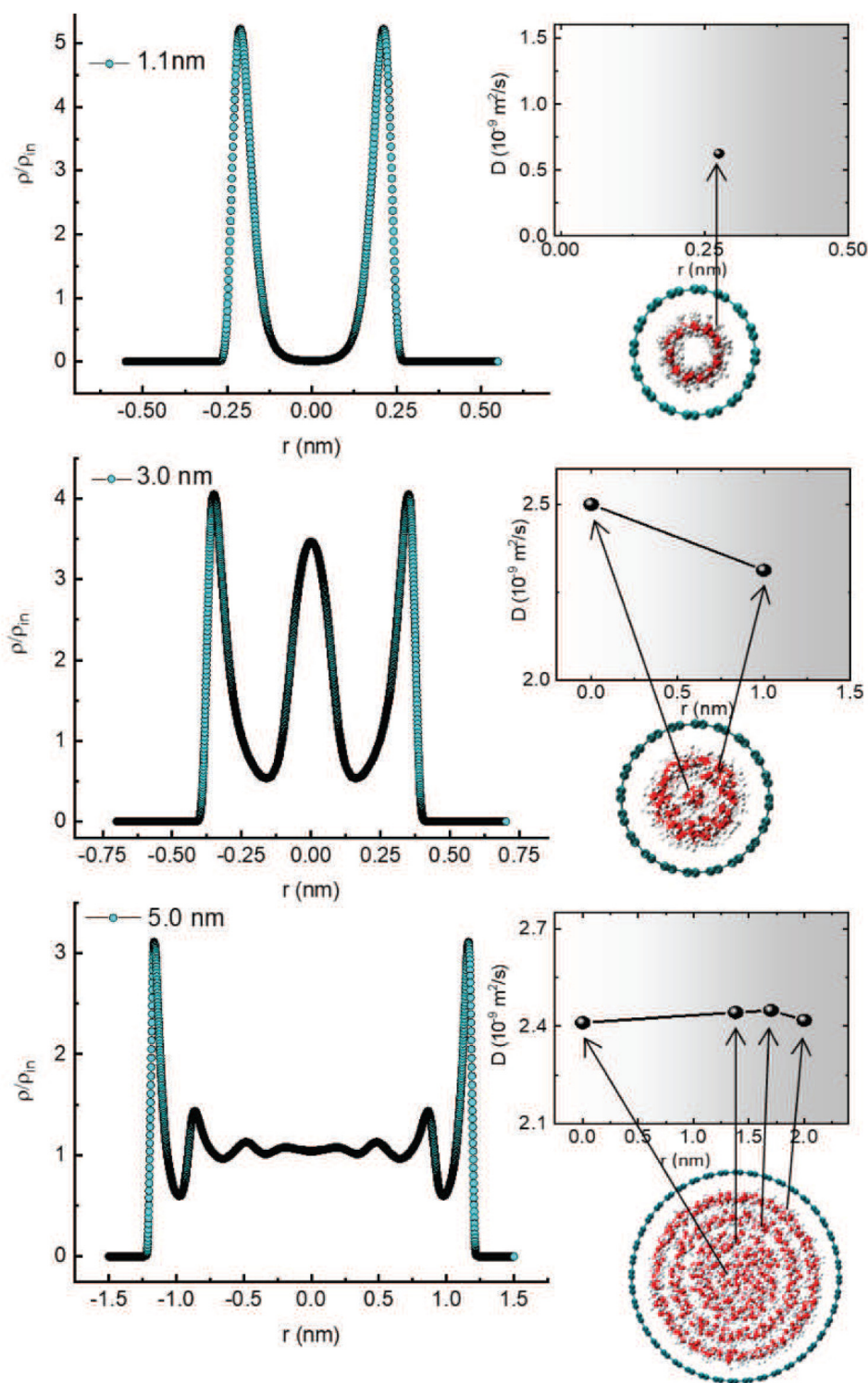
FIG. 4. Water local density inside different CNT sizes along with their corresponding models obtained using MD simulations, at room temperature. The x axis is the CNT inner diameter, where zero represents the center of the nanotube. Self-diffusion coefficients for the observed water layers inside CNTs were also calculated.
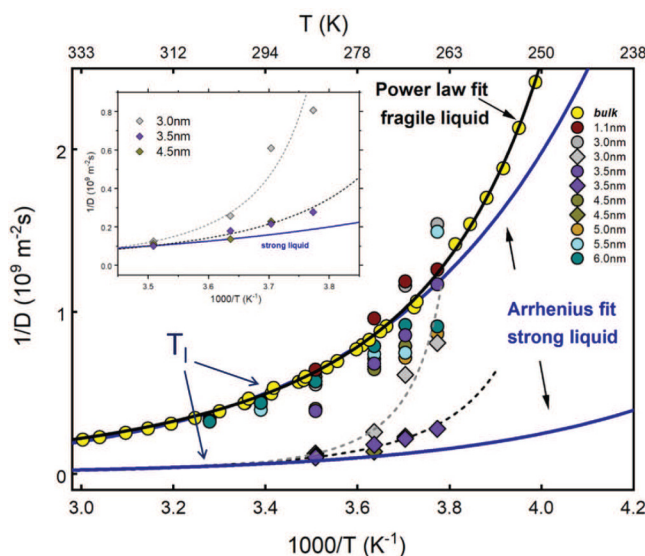
FIG. 5. Experimental $1/D$ vs $1000/T$ of the nanotube water in CNTs of various sizes. The blue lines (in both the main figure and the inset) are theoretical $1/D$ vs $1000/T$ curves of an ideal "strong" liquid obeying the Arrhenius law. The yellow circles and the black line are the experimental values of bulk water and the relevant power-law fit. In CNT sizes of 3.0, 3.5, and 4.5 nm, two water groups are resolved with different dynamics (slow and fast). The gray and the black dashed-lines are the power line fits of the data of the fast nanotube water group. The blue arrows are the relevant liquidus temperatures T_l. The inset is magnification of the $1/D$ vs $1000/T$ curves of the fast water component for CNT sizes 3.0, 3.5, and 4.5 nm. The self-diffusion data of bulk water at temperatures below 260 K were taken from Refs. 10 and 11 of the supplementary material.

completely liquid, strong deviation from the Arrhenius law is observed, while by approaching the glass-forming transition temperature, $1/D$ obeys the Arrhenius behavior again.[22] In our experiments, no evidence of the glass transition temperature for the water inside the nanotubes was found within the temperature range investigated, in accordance with previous works (for example, Ref. 22). The high temperature Arrhenius and non-Arrhenius dynamic crossover at the liquidus temperature T_l has been observed in many glass-forming systems.[53] Liquids with this kind of behavior are denoted as "fragile" liquids. Similar to the bulk water, the temperature dependence of the diffusion coefficient of nanotube water shows strongly non-Arrhenius behavior. Many theoretical explanations have been proposed to explain the fragile behavior of water, such as the change in the translational and reorientation dynamics,[54] the coexistence of high and low-density liquid structures,[55,56] the increasingly collective character of water motions at low temperatures,[57] the freezing of some collective motions,[58,59] and a connection of hydrogen bond exchange dynamics to local structural fluctuations.[60] For a quantitative description of our data, we adopted the Speedy–Angell power-law approach, having the following form:[61]

$$\frac{1}{D} = \frac{1}{D_0} \exp\left[\frac{T}{T_S} - 1\right]^{\gamma},$$

where T_S is the thermodynamic limit at which transport properties become zero,[62] and the exponent γ is associated with the fragility and the formation of an open hydrogen bond network.

In the case of bulk water, the solid black line is the power-law fit to the experimental data (yellow circles) with $T_S = 218\,\text{K}$ and $\gamma = -2$ in agreement with previously reported values.[63] Evidently, the adopted power law describes adequately the dynamical behavior of bulk water. In small and large CNT sizes (1.1 nm, 5.0 nm, 5.5 nm, and 6.0 nm), the nanotube water dynamics is similar to that of bulk water, while in the CNT size range 3.0–4.5 nm, two nanotube water groups are resolved with different dynamics, i.e., an outer slow component (circle data points) and a central fast one (rhombus data points). The data of the fast nanotube water group (rhombus) can be fitted to the Speedy–Angell power-law only when γ values in the range of −2.0 to −5.0 are considered. This indicates that the fast axial water component attains a very fragile structure,[45] resisting the formation of a hydrogen bonding network upon cooling. Besides, the liquidus temperature T_l of the fast water component shifts to higher temperatures, a behavior associated with the size dependent rise of the melting temperature in very narrow single-walled CNTs.[64,65] It is furthermore observed that in the specific size range (3.0–4.5 nm), the $1/D$ vs T curve of the slow water component deviates from that of bulk water; specifically, even the outer WTS close to the CNT walls acquires higher liquidus temperature and higher fragility than bulk water. This assignment differs from the picture conveyed by certain MD simulation reports,[11] where water close to the CNT walls is shown to diffuse faster due to pure hydrophobic interactions between the water and the CNT walls, a fact, however, which does not explain the dynamic spatial heterogeneity between the central and the outer WTS components revealed by our experiments.

Figure 6 shows the experimental D values at the maximum NMR signal intensity in Fig. 3, together with the relevant MD simulation results. At 285 K, a diffusion maximum is observed in the diameter range of 3.0–4.5 nm, as also shown in Fig. 3. The maximum D value decreases by lowering the temperature, indicating the freezing of the diffusion process. Similarly, the MD simulations (black points and black lines in Fig. 6) show at 300 K a discernible maximum, in relative agreement with previous MD results;[11] the smaller D values in our simulations in comparison to Ref. 11 might be due to slight differences in the boundary conditions used. However, no D maximum was observed in the MD simulations at other temperatures. Furthermore, the low D values in the 1.0 nm CNT is caused by the extreme confinement effect and was reported in early studies on water in small CNT sizes.[66,67]

Another important observation in Fig. 6 is that the position of the experimental diffusion peak depends strongly on both the temperature and the CNT size. The inset in Fig. 6 shows the position of the diffusion maximum D_{max}, in the T vs d (CNT diameter) diagram. The highest temperature of D_{max} is observed at $d = 3.5\,\text{nm}$. Evidently, this is linked with the anomalously high liquidus temperature observed in this material, which may be considered as an indicator of the onset of atomic scale controlled water dynamics[65] and dynamically heterogeneous fragility.[68,69] The substantial slowdown of the nanotube water dynamics by increasing the CNT size might be related to the fact that in large CNTs, more stratified water layers are formed as also confirmed by our MD results in
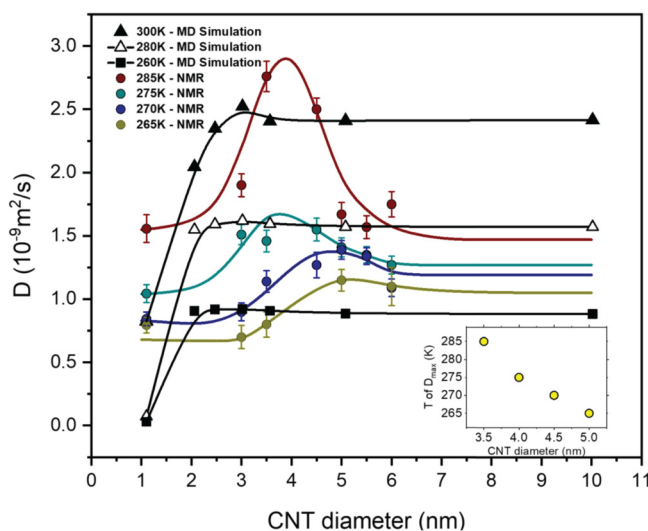
FIG. 6. The NMR self-diffusion coefficient D at the signal intensity peak in Fig. 3 vs the CNT size, at different temperatures (285 K, 275 K, 270 K, and 265 K). Black colored solid triangles, empty triangles, and solid squares are MD simulation results at 300 K, 280 K, and 260 K. The black solid lines are guides to the eye. The inset shows the CNT diameter of maximum diffusion (diffusion peak) at each measured temperature.

Fig. 4. It has been reported[10] that above four or five layers, the water gradually loses memory of the CNT wall and tends to acquire again the bulk water structure. Therefore, in large CNT channels, the structure of water molecules at the center of the tubes and the hydrogen bond network resemble that of the bulk water phase. The physical reasons behind the water diffusion enhancement, in particular, the CNT size (3.5 nm) in comparison to the diffusion in larger sizes (e.g., 5.5 nm), are still not well understood. Similar results were obtained by MD simulation[7,11,12] and experimental groups.[43,70] In general, two factors are expected to control the diffusion rate in various sizes of CNTs: the water structure inside the CNTs and eventual functional groups on the CNT walls. Structural and vibrational studies have shown that the water structure inside a certain CNT size (3.0 nm) acquires ice-like clusters,[51,71] exhibiting cooperative motion with high diffusion. In this scheme, water clusters can diffuse smoothly and fast into these nanochannels. Notably, neutron scattering experiments, combined with MD simulations,[23] have shown that even in CNTs with a diameter of approximately 1.4 nm, water splits into a liquid like central component and a more rigid water component close to the CNT walls. Evidently, the lower D measured with NMR at the smallest CNT size of approximately 1.0 nm is due to spatial restriction. On the other hand, at a larger CNT size, we presume a bulk-phase water structure, due to the large available space in the inner channels of CNTs. Furthermore, previous reports[72–75] suggested that the functionalization of CNTs with oxygen groups may reduce the water diffusion coefficient due to the preferential interaction between oxygenated sites and water molecules. To the best of our knowledge, this is the first experiment result reporting the existence of a CNT diameter range at which maximum

water diffusion occurs. A similar trend is obtained by the MD simulations in Fig. 6, in agreement with previous calculations.[7,9–11,70,76] On the other hand, MD simulations show a sufficiently lower D enhancement of the central axial water component in comparison to NMR. It is important, therefore, to emphasize the difficulty to quantitatively compare NMR experimental results with MD simulations because (i) dynamical properties reported in MD literature are heavily depending on the water models and potential wells used[10] and (ii) due to the computational power limitation, the time accessible to all MD works is in the range of ps to very few ns. On the other hand, in NMR, the accessible experimental time is typically 1–2 orders of magnitude longer than that of MD simulations. Nevertheless, MD simulations show similar trends with NMR, regarding water structure and dynamics in the CNT nanotubes, assisting in this way the analysis of the NMR experiments.

III. CONCLUSIONS

We have presented 2D NMR D–T_{2eff} results of water inside CNTs of different sizes and at various temperatures in combination with MD simulations. Our experiments show in a unique way the existence of a favorable CNT size range (3.0–4.5 nm) with anomalously enhanced water diffusion. In this size range, the nanotube water is further resolved into two components, with the central one exhibiting astonishing transport properties, with extraordinary high liquidus temperature T_l, and D values ranging from two to almost four times than the D values of the bulk water. Evidently, atomic scale interactions dominate water dynamics in this CNT diameter range giving rise to the heterogeneity in the fragile behavior between the central and the outer components of the confined water. The origin of this behavior can be traced to the interrelation between the strength of the repulsive part of the interatomic potential and the liquid fragility[77] as well as to the associated hydrogen bond lifetimes of water within the carbon nanotubes.[78] To the best of our knowledge, this is the first experiment result reporting on the existence of a CNT diameter range at which maximum water diffusion occurs and simultaneously exhibiting a size dependent liquid fragility. In general, the existence of new phases of water inside CNTs can add a new prospective in the field and it is an important finding on the design of nano-channels for membrane separation and drug delivery systems.

IV. MATERIALS AND METHODS

A. Materials

Purified carbon nanotubes, Single, Double, and Multiple (SWCNT, DWCNT, and MWCNT), were purchased from SES research, USA. The inner diameter of the CNTs used in this work was approximately 1.1 nm for the SWCNT, approximately 3.5 nm for the DWCNT, and approximately 4.5 nm for the MWCNT. Additionally, further MWCNT samples were purchased from Nanocs, USA with inner diameters 3.0, 5.0, 5.5, and 6.0 nm. The length of the tubes in all the CNTs used in this work was from 15 μm to 20 μm and all the CNTs were open ended as provided by the manufacturer. The samples were characterized using TEM-FEI Tecnai G20 with a 0.11 nm point to point resolution and found consistent with manufacturer's specifications. The CNT powder

was used with no further treatment and doubly distilled water was used for the NMR samples preparation. Further information on the CNTs and the preparation of the NMR samples is available in the supplementary material.

B. NMR experiments

2D ^{1}H NMR diffusion–relaxation D–T_{2eff} measurements were performed in the stray field of a 4.7 T Bruker superconductive magnet providing a 34.7 T/m constant magnetic field gradient at ^{1}H NMR frequency of 101.324 MHz. The experiments were carried out by using a pulse sequence with more than 5000 pulses (more details can be found in the supplementary material). The temperature was controlled by an ITC-5 temperature controller in a flow type Oxford cryostat. The accuracy of the temperature was 0.1 K. A 30 min time window was allowed at each temperature before collecting data. NMR data were analyzed using a 2D non-negative Tikhonov regularization inversion (discussed in the supplementary material) algorithm code developed by the authors.

C. Computational

Molecular dynamics simulations were used to investigate the diffusion of water inside single-walled carbon nanotubes. Different systems were simulated for CNTs with different diameters. Each system consists of a nanotube of length 20nm immersed in a water bath. The nanotubes studied were armchairs (4, 4), (8, 8), (15, 15), (18, 18), (22, 22), (26, 26), (37, 37), and (73, 73) of diameters 0.55 nm, 1.10 nm, 2.06 nm, 2.47 nm, 3.02 nm, 3.57 nm, 5.08 nm, and 10.02 nm correspondingly. The molecular dynamics simulations were implemented using NAMD40. Water molecule was represented using the Simple Point Charge/Extended (SPC/E) model, which predicts accurately many of the bulk water properties.[46] The non-bonded interactions between carbon atoms were modeled using the Lennard-Jones (LJ) potential with the parameters $epsilon = 0.069$ kcal/mol, $r_{min} = 3.805$ Å given by Werder et al.[8] The positions of the carbon atoms were held fixed throughout the simulations. The systems were kept at the same temperature of 300 K using Langevin Thermostat. In addition, the pressure was maintained at 1.0 atm using Nosé–Hoover Langevin piston with a period of 100 fs and a damping time scale of 50 fs. The simulations were performed using periodic boundary conditions in which electrostatic interactions were calculated using Particle Mesh Ewald (PME). The simulation integration time step was 2.0 fs. Bonded interactions were calculated every time step while non-bonded interaction was calculated every two steps with a cutoff of 12 Å and switching function of 10 Å. All simulated systems were minimized for 10 000 steps and then gradually heated to the target temperature of 300 K. Each system was then equilibrated at 300 K for 50 000 steps (100 ps) before the production runs. The production simulations were run for a total time of 50 ns. The system configuration was saved every 500 steps (1.0 ps) for analysis. The water density profile was calculated for each simulated system inside the CNTs in order to elucidate the structure. The self-diffusion coefficient was determined using the mean squared displacement function (MSD) in the axial direction. MSD is calculated over a time interval of 1.0 ns at a sampling rate of 1 ps. MSD was then averaged over 50 such time intervals. The interval length, 1.0 ns, was chosen carefully to give water molecule

enough time inside the carbon nanotube before exiting. In order to estimate the diffusion constant D, we fit the later part of MSD function ($MSD_{t\to\infty} = 2Dt$) to a straight line using simple least squares regression model ($\beta_0 + \beta_1 t$). The estimated slope ($\hat{\beta}_1$) is equal to two times the diffusion coefficient ($2D$). In order to estimate the error in D (approximately 10^{-12} m^2/s), we used the estimated standard error of the slope $\hat{\beta}_1 = \frac{\sqrt{MSE}}{S_{xx}}$. The diffusion coefficients were calculated for all of the water inside the CNT and for all the components obtained from the density profile.

SUPPLEMENTARY MATERIAL

See the supplementary material for the (1) materials and methods, (2) 2D ^{1}H NMR D–T_{2eff} measurements, (3) comparison between simulated and experimental ^{1}H NMR diffusion measurements, (4) T_{2eff} projections at different temperatures, (5) analysis of strong and fragile liquids, and (6) molecular dynamics simulation details.

DATA AVAILABILITY

The data that support the findings of this study are available within the article and its supplementary material. Further data are available from the corresponding authors upon reasonable request.

REFERENCES

[1]R. Das, M. E. Ali, S. B. A. Hamid, S. Ramakrishna, and Z. Z. Chowdhury, "Carbon nanotube membranes for water purification: A bright future in water desalination,' Desalination **336**, 97–109 (2014).
[2]S. Ketabi and L. Rahmani, "Carbon nanotube as a carrier in drug delivery system for carnosine dipeptide: A computer simulation study," Mater. Sci. Eng. C **73**, 173–181 (2017).
[3]W. Zhang, Z. Zhang, and Y. Zhang, "The application of carbon nanotubes in target drug delivery systems for cancer therapies," Nanoscale Res. Lett. **6**, 555 (2011).
[4]P. M. Costa, M. Bourgognon, J. T. W. Wang, and K. T. Al-Jamal, "Functionalised carbon nanotubes: From intracellular uptake and cell-related toxicity to systemic brain delivery," J. Control. Release **241**, 200–219 (2016).
[5]S.-B. Ma, K.-W. Nam, W.-S. Yoon, X.-Q. Yang, K.-Y. Ahn, K.-H. Oh, and K.-B. Kim, "Electrochemical properties of manganese oxide coated onto carbon nanotubes for energy-storage applications," J. Power Sources **178**, 483–489 (2008).
[6]Y. H. Lee, K. H. An, S. C. Lim, W. S. Kim, H. J. Jeong, C.-H. Doh, and S.-I. Moon, "Application of carbon nanotubes to energy storage devices," New Diamond Front. Carbon Technol. **12**, 209–228 (2002).
[7]A. Alexiadis and S. Kassinos, "Self-diffusivity, hydrogen bonding and density of different water models in carbon nanotubes," Mol. Simul. **34**, 671–678 (2008).

[8] T. Werder, J. H. Walther, R. Jaffe, T. Halicioglu, and P. Koumoutsakos, "On the water–carbon interaction for use in molecular dynamics simulations of graphite and carbon nanotubes," Phys. Chem. B **107**, 1345–1352 (2003).

[9] J. R. Bordin, A. Diehl, and M. C. Barbosa, "Relation between flow enhancement factor and structure for core-softened fluids inside nanotubes," J. Phys. Chem. B **117**, 7047–7056 (2013).

[10] A. Alexiadis and S. Kassinos, "Molecular simulation of water in carbon nanotubes," Chem. Rev. **108**, 5014–5034 (2008).

[11] A. Barati-Farimani and N. R. Aluru, "Spatial diffusion of water in carbon nanotubes: From Fickian to ballistic motion," J. Phys. Chem. B **115**, 12145–12149 (2011).

[12] J. K. Holt, H. G. Park, Y. Wang, M. Stadermann, A. B. Artyukhin, C. P. Grigoropoulos, A. Noy, and O. Bakajin, "Fast mass transport through sub-2-nanometer carbon nanotubes," Science **312**, 1034-1037 (2006).

[13] J. Chen, M. A. Hamon, H. Hu, Y. Chen, A. M. Rao, P. C. Eklund, and R. C. Haddon, "Solution properties of single-walled carbon nanotubes," Science **282**, 95–98 (1998).

[14] A. Kukovecz, C. Kramberger, V. Georgakilas, M. Prato, and H. Kuzmany, "A detailed Raman study on thin single-wall carbon nanotubes prepared by the HiPCO process," Eur. Phys. J. B **28**, 223–230 (2002).

[15] S. Campidelli, M. Meneghetti, and M. Prato, "Separation of metallic and semiconducting single-walled carbon nanotubes via covalent functionalization," Small **3**, 1672–1676 (2007).

[16] B. J. Landi, C. D. Cress, C. M. Evans, and R. P. Raffaelle, "Thermal oxidation profiling of single-walled carbon nanotubes," Chem. Mater. **17**, 6819–6834 (2005).

[17] D. Bonifazi, C. Nacci, R. Marega, S. Campidelli, G. Ceballos, S. Modesti, M. Meneghetti, and M. Prato, "Microscopic and spectroscopic characterization of paintbrush-like single-walled carbon nanotubes," Nano Lett. **6**, 1408–1414 (2006).

[18] Y. Gogotsi, J. A. Libera, and M. Yoshimura, "Hydrothermal synthesis of multi-wall carbon nanotubes," J. Mater. Res. **15**, 2591–2594 (2000).

[19] Y. Gogotsi, J. A. Libera, A. Guvenc-Yazicioglu, and C. M. Megaridis, "In situ multiphase fluid experiments in hydrothermal carbon nanotubes," Appl. Phys. Lett. **79**, 1021–1023 (2001).

[20] N. Naguib, H. Ye, Y. Gogotsi, A. Guvenc-Yazicioglu, C. M. Megaridis, and M. Yoshimura, "Observation of water confined in nanometer channels of closed carbon nanotubes," Nano Lett. **4**, 2237–2243 (2004).

[21] H. Ye, N. Naguib, and Y. Gogotsi, "TEM study of water in carbon nanotubes," JEOL News **39**, 38–43 (2004).

[22] X.-Q. Chu, A. I. Kolesnikov, A. P. Moravsky, V. Garcia-Sakai, and S.-H. Chen, "Observation of a dynamic crossover in water confined in double-wall carbon nanotubes," Phys. Rev. E **76**, 021505 (2007).

[23] A. I. Kolesnikov, J.-M. Zanotti, C.-K. Loong, P. Thiyagarajan, A. P. Moravsky, R. O. Loutfy, and C. J. Burnham, "Anomalously soft dynamics of water in a nanotube: A revelation of nanoscale confinement," Phys. Rev. Lett. **93**, 3035503 (2004).

[24] E. Mamontov, C. J. Burnham, S.-H. Chen, A. P. Moravsky, C.-K. Loong, N. R. de Souza, and A. I. Kolesnikov, "Dynamics of water confined in single-and double-wall carbon nanotubes," J. Chem. Phys. **124**, 194703 (2006).

[25] G. Briganti, G. Rogati, A. Parmentier, M. Maccarini, and F. D. Luca, "Neutron scattering observation of quasi-free rotations of water confined in carbon nanotubes," Sci. Rep. **7**, 45021 (2017).

[26] G. Hummer, J. C. Rasaiah, and J. P. Noworyta, "Water conduction through the hydrophobic channel of a carbon nanotube," Nature **414**, 6860 (2001).

[27] D. J. Bonthuis, K. F. Rinne, K. Falk, C. N. Kaplan, D. Horinek, A. N. Berker, L. Bocquet, and R. R. Netz, "Theory and simulations of water flow through carbon nanotubes: Prospects and pitfalls," J. Phys. Condens. Matter **23**, 18 (2011).

[28] S. Mondal and B. Bagchi, "Water in carbon nanotubes: Pronounced anisotropy in dielectric dispersion and its microscopic origin," J. Phys. Chem. Lett. **10**, 20 (2019).

[29] G. F. Reiter, A. Deb, Y. Sakurai, M. Itou, V. G. Krishnan, and S. J. Paddison, "Anomalous ground state of the electrons in nanoconfined water," Phys. Rev. Lett. **111**, 036803 (2013).

[30] G. F. Reiter, A. Deb, Y. Sakurai, M. Itou, and A. I. Kolesnikov, "Quantum coherence and temperature dependence of the anomalous state of nanoconfined water in carbon nanotubes," J. Chem. Phys. Lett. **7**, 4433–4437 (2016).

[31] Y. Maniwa, H. Kataura, M. Abe, S. Suzuki, Y. Achiba, H. Kira, and K. Matsuda, "Phase transition in confined water inside carbon nanotubes," J. Phys. Soc. Jpn. **71**, 12 (2002).

[32] M. Perez-Cabero, I. Rodriguez-Ramos, A. Overweg, I. Sobrados, J. Sanz, and A. Guerrero-Ruiz, "^{13}C MAS-NMR study of carbon nanotubes grown by catalytic decomposition of acetylene on Fe-silica catalysts," Carbon **43**, 2631–2634 (2005).

[33] M. Urbán, Z. Kónya, D. Méhn, and I. Kiricsi, "IR and NMR spectroscopic characterization of graphitization process occurring in the pores of mesoporous silicates in formation of carbon nanotubes," J. Mol. Struct. **744–747**, 93–99 (2005).

[34] J. L. Blackburn, Y. Yan, C. Engtrakul, P. A. Parilla, K. Jones, T. Gennett, A. C. Dillon, and M. J. Heben, "Synthesis and characterization of boron-doped single-wall carbon nanotubes produced by the laser vaporization technique," Chem. Mater. **18**, 2558–2566 (2006).

[35] E. Abou-Hamad, M.-R. Babaa, M. Bouhrara, Y. Kim, Y. Saih, S. Dennler, F. Mauri, J.-M. Basset, C. Goze-Bac, and T. Wågberg, "Structural properties of carbon nanotubes derived from ^{13}C NMR," Phys. Rev. B **84**, 165417 (2011).

[36] J. Hassan, G. Diamantopoulos, D. Homouz, and G. Papavassiliou, "Water inside carbon nanotubes: Structure and dynamics," Nanotechnol. Rev. **5**, 341–354 (2016).

[37] R. Böhmer and C. A. Angell, "Disorder effects on relaxational processes," in Local and Global Relaxations in Glass Forming Materials, edited by R. Richert and A. Blumen (Springer, Berlin, 1994).

[38] K. Matsuda, T. Hibi, H. Kadowaki, H. Kataura, and Y. Maniwa, "Water dynamics inside single-wall carbon nanotubes: NMR observations," Phys. Rev. B **74**, 073415 (2006).

[39] H. Kyakuno, K. Matsuda, H. Yahiro et al., "Confined water inside single-walled carbon nanotubes: Global phase diagram and effect of finite length," J. Chem. Phys. **134**, 244501 (2011).

[40] A. Das, S. Jayanthi, H. S. M. V. Deepak, K. V. Ramanathan, A. Kumar, C. Dasgupta, and A. K. Sood, "Single-file diffusion of confined water inside SWNTs: An NMR study," ACS Nano **4**, 1687–1695 (2010).

[41] S. Ghosh, K. V. Ramanathan, and A. K. Sood, "Water at nanoscale confined in single-walled carbon nanotubes studied by NMR," Europhys. Lett. **65**, 678–684 (2004).

[42] W. Sekhaneha, M. Kotecha, U. Dettlaff-Weglikowska, and W. S. Veeman, "High resolution NMR of water absorbed in single-wall carbon nanotubes," Chem. Phys. Lett. **428**, 143–147 (2006).

[43] X. Liu, X. Pan, S. Zhang, X. Han, and X. Bao, "Diffusion of water inside carbon nanotubes studied by pulsed field gradient NMR spectroscopy," Langmuir **30**, 8036–8045 (2014).

[44] H.-J. Wang, X.-K. Xi, A. Kleinhammes, and Y. Wu, "Temperature-induced hydrophobic–hydrophilic transition observed by water adsorption," Science **322**, 80–83 (2008).

[45] J. Hassan, G. Diamantopoulos, L. Gkoura et al., "Ultrafast stratified diffusion of water inside carbon nanotubes; direct experimental evidence with 2D D−T$_2$ NMR spectroscopy," J. Phys. Chem. C **122**, 10600–10606 (2018).

[46] J. C. Phillips, R. Braun, W. Wang, J. Gumbart, E. Tajkhorshid, E. Villa, C. Chipot, R. D. Skeel, L. Kalé, and K. Schulten, "Scalable molecular dynamics with NAMD," J. Comput. Chem. **26**, 1781–1802 (2005).

[47] H. J. C. Berendsen, R. Grigera, and P. Straatsma, "The missing term in effective pair potentials," J. Phys. Chem. **91**, 6269–6271 (1987).

[48] R. Kimmich, W. Unrath, G. Schnur, and E. Rommel, "NMR measurement of small self-diffusion coefficients in the fringe field of superconducting magnets," J. Magn. Reson. **91**, 136–140 (1991).

[49] M. D. Hürlimann, L. Venkataramanan, and C. Flaum, "The diffusion–spin relaxation time distribution function as an experimental probe to characterize fluid mixtures in porous media," J. Chem. Phys. **117**, 10223–10232 (2002).

[50]P. T. Callaghan, K. W. Jolley, and J. Lelievre, "Diffusion of water in the endosperm tissue of wheat grains as studied by pulsed field gradient nuclear magnetic resonance," Biophys. J. **28**, 133–141 (1979).

[51]T. Ohba, K. Kaneko, M. Endo, K. Hata, and H. Kanohl, "Rapid water transportation through narrow one-dimensional channels by restricted hydrogen bonds," Langmuir **29**, 1077–1082 (2013).

[52]R. Shi, J. Russo, and H. Tanaka, "Origin of the emergent fragile-to-strong transition in supercooled water," Proc. Natl. Acad. Sci. U.S.A. **115**, 9444–9449 (2018).

[53]T. Wen, W. Yao, and N. Wang, "Correlation between the Arrhenius crossover and the glass forming ability in metallic glasses," Sci. Rep. **7**, 13164 (2017).

[54]D. Rozmanov and P. G. Kusalik, "Transport coefficients of the TIP4P-2005 water model," J. Chem. Phys. **136**, 044507 (2012).

[55]P. K. L. Xu, S. V. Buldyrev, S.-H. Chen, P. H. Poole, F. Sciortino, and H. E. Stanley, "Relation between the Widom line and the dynamic crossover in systems with a liquid–liquid phase transition," Proc. Natl. Acad. Sci. U.S.A. **102**, 16558–16562 (2005).

[56]C. Huang, K. T. Wikfeldt, T. Tokushima, D. Nordlund, Y. Harada, U. Bergmann, M. Niebuhr, T. M. Weiss, Y. Horikawa, M. Leetmaa *et al.*, "The inhomogeneous structure of water at ambient conditions," Proc. Natl. Acad. Sci. U.S.A. **106**, 15214–15218 (2009).

[57]R. A. Nicodemus, S. A. Corcelli, J. L. Skinner, and A. Tokmakoff, "Collective hydrogen bond reorganization in water studied with temperature-dependent ultrafast infrared spectroscopy," J. Phys. Chem. B **115**, 5604–5616 (2011).

[58]P. Gallo, F. Sciortino, P. Tartaglia, and S.-H. Chen, "Slow dynamics of water molecules in supercooled states," Phys. Rev. Lett. **76**, 2730–2733 (2011).

[59]J. Swenson and J. Teixeira, "The glass transition and relaxation behavior of bulk water and a possible relation to confined water," J. Chem. Phys. **132**, 014508 (2010).

[60]G. Stirnemann and D. Laage, "Communication: On the origin of the non-Arrhenius behavior in water reorientation dynamics," J. Chem. Phys. **137**, 031101 (2012).

[61]R. Speedy and C. Angell, "Isothermal compressibility of supercooled water and evidence for a thermodynamic singularity at $-45\,°C$," J. Chem. Phys. **65**, 851–858 (1976).

[62]K. L. Ngai, *Relaxation and Diffusion in Complex Systems: Partially Ordered Systems* (Springer Science & Business Media LLC, 2011), ISBN: 978-1-4419-7648-2.

[63]F. Perakis and P. Hamm, "Two-dimensional infrared spectroscopy of supercooled water," J. Phys. Chem. B **115**, 5289–5293 (2011).

[64]Y. Maniwa, H. Kataura, M. Abe, A. Udaka, S. Suzuki, Y. Achiba, H. Kira, K. Matsuda, H. Kadowaki, and Y. Okabe, "Ordered water inside carbon nanotubes: Formation of pentagonal to octagonal ice-nanotubes," Chem. Phys. Lett. **401**, 534–538 (2005).

[65]M. M. C. P. Pugliese, M. Rovere, and P. Gallo, "Freezing temperatures, ice nanotubes structures, and proton ordering of TIP4P/ice water inside single wall carbon nanotubes," J. Phys. Chem. B **121**, 10371–10381 (2017).

[66]S. J. R. J. Mashl, N. R. Aluru, and E. Jakobsson, "Anomalously immobilized water: A new water phase induced by confinement in nanotubes," Nano Lett. **3**, 589-592 (2003).

[67]G. Zuo, S. M. R. Shen, and W. Guo, "Transport properties of single-file water molecules inside a carbon nanotube biomimicking water channel," ACS Nano **4**, 205–210 (2010).

[68]R. Richert, "Heterogeneous dynamics in liquids: Fluctuations in space and time," J. Phys. Condens. Matter **14**, R703–R738 (2002).

[69]N. R. D. Souza, A. I. Kolesnikov, C. J. Burnham, and C.-K. Loong, "Structure and dynamics of water confined in single-wall carbon nanotubes," J. Phys. Condens. Matter **18**, S2321–S2334 (2006).

[70]K. I. T. Ohba, K. Hata, S. H. Yoon, J. Miyawaki, and K. Hata, "Fast water relaxation through one-dimensional channels by rapid energy transfer," ChemPhysChem **17**, 3409–3415 (2016).

[71]T. Ohba, "Size-dependent water structures in carbon nanotubes," Angew. Chem. **126**, 8170–8174 (2014).

[72]A. Striolo, "Water self-diffusion through narrow oxygenated carbon nanotubes," Nanotechnology **18**, 475704 (2007).

[73]M. Majumder and B. Corry, "Anomalous decline of water transport in covalently modified carbon nanotube membranes," Chem. Commun. **47**, 683–7685 (2011).

[74]B. Corry, "Water and ion transport through functionalised carbon nanotubes: Implications for desalination technology," Energy Environ. Sci. **4**, 751–759 (2011).

[75]M. Majumder, N. Chopra, and B. J. Hinds, "Mass transport through carbon nanotube membranes in three different regimes: Ionic diffusion and gas and liquid flow," ACS Nano **5**, 3867–3877 (2011).

[76]H. Ye, H. Zhang, Y. Zheng, and Z. Zhang, "Nanoconfinement induced anomalous water diffusion inside carbon nanotubes," Microfluid. Nanofluid. **10**, 1359–1364 (2011).

[77]C. E. Pueblo, M. Sun, and K. F. Kelton, "Strength of the repulsive part of the interatomic potential determines fragility in metallic liquids," Nat. Mater. **16**, 792–796 (2017).

[78]I. Hanasaki and A. Nakatani, "Hydrogen bond dynamics and microscopic structure of confined water inside carbon nanotubes," J. Chem. Phys. **124**, 174714 (2006).